Appl. Phys. B 54, 443–450 (1992)

Applied Physics B Photophysics and Laser Chemistry

Multiphoton Resonances in Atomic Bragg Scattering

M. Marte* and S. Stenholm

Research Institute for Theoretical Physics, Siltavuorenpenger 20 C, SF-00170 Helsinki, Finland, Fax: (+358-0/1918366)

Received 21 October 1991/Accepted 17 December 1991

Abstract. We investigate the atomic scattering from a standing-wave light beam in the Bragg regime. Here momentum conservation requires the scattering to flip between two allowed directions only. In this limit an adiabatic approximation allows us to obtain analytic expressions for the flipping. The various orders of such resonances are compared with the multiphoton resonances observed in radio-frequency spectra, when they are interpreted in terms of Dopplerons. In addition to the main frequency of flipping, we find a modulation of the whole beam, which is seen when the scattered beam interferes with some differently prepared component of itself. We integrate the coupled equations numerically and find that the adiabatic approximation gives a good description of the processes over a large range of parameter values.

PACS: 42.50.Dv, 42.50.Vk

When an atomic beam traverses the beam of a monochromatic standing wave, the internal quantum states may absorb and emit photons assuming that the laser is tuned nearly into resonance with some atomic transition. Momentum conservation requires that the photon momentum is manifested in a change of the translational state of the atom. If the standing wave is decomposed into its travelling wave components, the atom may hence be deflected in the direction of wave propagation by any integer number of photon momenta; the physical situation is shown in Fig. 1. Another point of view assigns the momentum spreading to the umklapp processes deriving from the periodic potential offered by the standing wave to the atom. The process is equivalent with the Kapitza-Dirac effect for electrons, but with atoms the scattering can be enhanced by the resonant nature of the energy transfer. In view of the recent interest in atomic interferometric configurations, the diffractive atomic scattering has aquired new actuality.

The first experimental investigations of atomic beam spreading by a standing wave were carried out by Arimondo and Oka [1] and Grinchuk et al. [2]. However, these works lacked the resolution to see the individual diffraction peaks in the scattering. These were first seen by Pritchard and his collaborators [3]. They have also been able to follow the phenomenon into its various regimes [4]. The simplest theory assumes the time evolution to be entirely unitary, but relaxation processes have been introduced into the theory in [5–7]. Experimentally the transition regime has been investigated by Pritchard's group [8].

In the optical regime one always performs the rotating-wave-approximation and only consecutive excitation-deexcitation processes are possible. In a standing wave, however, these can utilize photons from both travelling wave components, which implies that the atom may return to the ground state with twice the Doppler shift characteristic of the one-photon process. For strong fields many translational states become superimposed which causes diffractive scattering. The Doppler shifts can be accumulated in an additive fashion, when absorption-emission sequences use photons from alternate travelling wave components. When the laser is detuned, these can be utilized to compensate the energy mismatch between the photon and the atomic transition. Thus, in an N photon process, we may pick up N units of Doppler shifts to achieve a resonant transition. In [9] we used this fact to introduce a fictitious particle, the Doppleron, carrying the energy of one Doppler shift. The situation is analogous to that in radio-frequency spectroscopy, where one must include the counter-rotating term in the interaction. This allows the possibility to achieve multiphoton resonant transitions by the absorption of several quanta of the radio-frequency field. To reach the upper state an odd number is required. Such calculations were

* Permanent address: Institut für Theoretische Physik, Universität Innsbruck, A-6020 Innsbruck, Austria

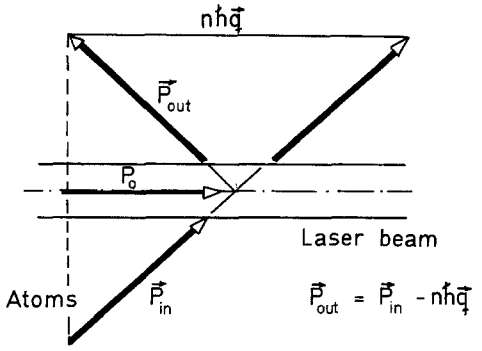

Fig. 1. Geometric configuration showing the conservation of momentum in atomic Bragg scattering from a standing light wave

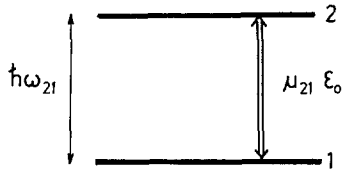

Fig. 2. Dipole transitions induced in a two-level atom interacting with a classical field

first carried out by Winter [10] and pursued systematically by Cohen-Tannoudji [11] and Haroche [12].

Atomic scattering from a standing wave can be classified into two main parameter regimes, the Raman-Nath and the Bragg regime. In the latter, energy conservation plays an essential role and restricts the possible deflection angels just as in X-ray scattering from a crystal. In this regime, the scattering displays the pendellösung phenomenon [13], which is known from neutron scattering, too.

In this paper we point out that the various orders of scattering in the Bragg regime display an analogy with the multiphoton resonances in radiofrequency spectroscopy, when the processes are interpreted in accordance with the Doppleron analogy. The original treatment [9] did not include atomic recoil, and hence, we have to generalize the treatment to satisfy energy conservation. This is done in Sect. 1, where we derive the basic equations to be used in the paper.

In Sect. 2 we discuss the Bragg regime and the multiphoton interpretation of the resonances. Asymptotically, the phenomena can be discussed in an adiabatic approximation, which gives an analytic expression for the oscillation frequency of any pendellösung behaviour. It turns out, however, that another frequency emerges out of the treatment, which modulates the state vector of the atom. If only the different orders of momentum deflection are monitored, this factor is not observed, but as soon as the atomic beam interfers with some differently prepared component of itself, this frequency will be seen. In the different orders of scattering, the two frequencies scale differently with the strength of the light field, and hence, they appear in different ways in different observables.

We have also carried out numerical computations to check the validity of the analytical treatment, and in Sect. 3 these two approaches are discussed and compared. There, the special features of the two types of frequencies encountered receive additionally illumination. Finally, the work is summarized and discussed in Sect. 4.

1 Formulation of the Problem

The system under investigation is going to be represented by the two-level atom shown in Fig. 2. Its Hamiltonian can be written in the form

$$H = T_{\text{atom}} + \hbar\omega_{21}\,|2><2| - \mathbf{D}\cdot\mathbf{E}(x)\,. \tag{1}$$

Here T_{atom} is the kinetic energy of the center-of-mass, the field $\mathbf{E}(x)$ is assumed to be classical, and the dipole coupling operator is defined by

$$\mathbf{D}\cdot\vec{\varepsilon} = \hbar\mu_{21}(|1><2| + |2><1|)\,. \tag{2}$$

We write an ansatz for the state of the atom including its center-of-mass motion in the form

$$|\Psi> = \psi_2(x)\,e^{-i\omega t}|2> + \psi_1(x)|1>\,. \tag{3}$$

The laser field $\mathbf{E}(x)$ is assumed to be monochromatic enough to be characterized by the single frequency ω. Using (3) and (1) we obtain the Schrödinger equation

$$i\frac{\partial}{\partial t}\begin{bmatrix}\psi_2(x)\\ \psi_1(x)\end{bmatrix} = \begin{bmatrix}\Delta - \dfrac{\hbar}{2m}\dfrac{\partial^2}{\partial x^2} & -\mu_{21}\mathscr{E}(x)\\ -\mu_{21}\mathscr{E}(x) & -\dfrac{\hbar}{2m}\dfrac{\partial^2}{\partial x^2}\end{bmatrix}\begin{bmatrix}\psi_2(x)\\ \psi_1(x)\end{bmatrix}. \tag{4}$$

The rotating wave approximation introduces the field amplitudes $\mathscr{E}(x)$ as the coefficients of the exponentials $e^{\pm i\omega t}$; for simplicity they are assumed real. $\Delta = \omega_{21} - \omega$ is the detuning. For a simple standing wave we have

$$\mathscr{E}(x) = \mathscr{E}_0 \cos qx\,, \tag{5}$$

but our treatment is easily extended to more complicated, possibly 3-dimensional configurations. However, in this paper we are going to restrict the treatment to the one-dimensional case given by (5).

The momentum exchange structure induced by the simple standing wave (5) is most clearly displayed by an expansion in momentum eigenstates. The field in (5) then acquires the form

$$\mathscr{E}(x) = \tfrac{1}{2}\mathscr{E}_0 \exp\left(-q\frac{\partial}{\partial p}\right) + \text{h.c.}\,. \tag{6}$$

Starting from an initial atomic momentum p_0, the operator (6) mixes in only the components $p_0 + n\hbar q$, where n is any integer. For the coefficients in the ansatz (3) we introduce the momentum expansion

$$\psi_i(x) = \exp\left[i\left(\frac{p_0 x}{\hbar} - \frac{p_0^2}{2m\hbar}t\right)\right] \times \sum_{n=-\infty}^{\infty} e^{inqx} C_i(n); \tag{7}$$

when the atom enters in the lower level, the sum changes to even values of n for $i=1$ and odd ones for $i=2$. The prefactor is a Galilean transformation to the frame

moving with the initial momentum p_0 in the direction of the laser beam. It is included because it simplifies the equations.

Inserting (7) into (4) we obtain

$$\mathrm{i}\frac{d}{dt}C_1(n)=(W_0 n+\varepsilon n^2)\ C_1(n) -\tfrac{1}{2}\mu_{21}\mathscr{E}_0[C_2(n+1)+C_2(n-1)],$$

$$\mathrm{i}\frac{d}{dt}C_2(n)=(W_0 n+\varepsilon n^2+\Delta)\ C_2(n) -\tfrac{1}{2}\mu_{21}\mathscr{E}_0[C_1(n+1)+C_1(n-1)]. \quad (8)$$

We have introduced the initial Doppler shift of the atomic motion

$$W_0=\frac{p_0}{m}q=qv_0 \quad (9)$$

and the single photon recoil energy is

$$\hbar\varepsilon=\frac{\hbar^2q^2}{2m}. \quad (10)$$

When ε is neglected, the n-dependence of (8) is analogous to that of a harmonic motion with frequency W_0. This is the basis for the interpretation of the expression (7) as an expansion in terms of n-particle states called Dopplerons. They were introduced in [9] and have recently been explored experimentally [14].

The simplest case of diffractive scattering can be achieved when the recoil energy is smaller than the Rabi frequency coupling the two levels

$$\varepsilon\ll\Omega\equiv\tfrac{1}{2}\mu_{21}\mathscr{E}_0. \quad (11)$$

This limit is called the Raman-Nath regime. When ε is set to zero and the atom is tuned to resonance, $\Delta=0$, we can obtain the analytic solution for (8) (see [15])

$$C_i(n)=\exp\left[-\frac{\mathrm{i}}{2}\left(W_0t+\pi\right)n\right]J_n\left(\frac{4\Omega}{W_0}\sin\frac{W_0t}{2}\right), \quad (12)$$

($i=1$ or 2 for even or odd n, respectively). Here J_n is the n$-th$ Bessel function. This represents the diffractive scattering into the many momentum components $p_0+n\hbar q$ of the periodic potential offered by the standing wave. Experimental verification of scattering in this regime has been given in [4].

2 Multiphoton resonances in the Bragg Regime

Efficient use of a standing wave as a beam splitter or a deflector presumes that the atomic beam can be directed into one or a few directions only. This can be achieved in the so called Bragg regime which is complementary to the situation of (11)

$$\varepsilon\gg\Omega\equiv\tfrac{1}{2}\mu_{21}\mathscr{E}_0. \quad (13)$$

In this case, conservation of the kinetic energy becomes important in contrast to the situation in the Raman-Nath regime, which considers only momentum conservation. Now only those diffractive scattering processes, where energy is conserved together with momentum can be realized. For an interaction time of Δt, energy is conserved to within the uncertainty $\hbar/\Delta t$. The situation is depicted in Fig. 1, where we can see that the scattering events with

$$\mathbf{p}_{\mathrm{out}}=\mathbf{p}_{\mathrm{in}}-n\hbar\mathbf{q} \quad (14)$$

conserve the momentum of the atom. At resonance for the atomic transition ($\Delta=0$), conservation of the kinetic energy requires that $|\mathbf{p}_{\mathrm{out}}|=|\mathbf{p}_{\mathrm{in}}|$. In the equations of motion (8) this assumes that we have resonances between the two solutions of the equation

$$W_0n+\varepsilon n^2=0. \quad (15)$$

The solution $n=0$ corresponds to the incoming beam, and the other one

$$n=-n_0\equiv-\frac{W_0}{\varepsilon}=-\frac{2p_0}{\hbar q} \quad (16)$$

gives the scattered component conserving energy and momentum. Looking at Fig. 1 we find that the projection of the incoming and outgoing momenta must satisfy

$$p_0=\frac{\hbar q}{2}n \quad (17)$$

which corresponds to the Bragg condition in X-ray scattering from crystals.

In the set of secular equations (8) two zero oscillational frequencies occur on the diagonal of the Hamiltonian matrix. These signify multi-photon resonances between the two corresponding scattering directions. This is similar to the multiphoton situation encountered in radio-frequency spectroscopy [16]. In the present case, the photons are also real, but in the rotating wave approximation they carry only the Doppler energy $\hbar W_0$. They are Dopplerons.

When the resonance condition (16) is satisfied we can introduce the integer n_0 into (8) and write the coupled equations in the form

$$\mathrm{i}\,\underline{\dot{C}_2(1)}=\varepsilon(n_0+1)\ C_2(1)-\Omega\,\underline{[C_1(2)}+C_1(0)], \quad (18a)$$

$$\mathrm{i}\,\dot{C}_1(0)=-\Omega\,[C_2(1)+C_2(-1)], \quad (18b)$$

$$\mathrm{i}\,\underline{\dot{C}_2(-1)}=-\varepsilon(n_0-1)\ C_2(1)-\Omega\,[C_1(-2)+C_1(0)] \quad (18c)$$

etc.

For $n=-n_0$, we find the second vanishing of the diagonal term in the equations; this occurs for C_1 if n_0 is even and for C_2 if n_0 is odd. Let k denote the value 1 or 2 if n_0 is even or odd, respectively, and j is correspondingly 2 or 1. Then we find the equations

$$\mathrm{i}\,\underline{\dot{C}_j(-n_0+1)}=-\varepsilon(n_0-1)\ C_j(-n_0+1) -\Omega\,[C_k(-n_0+2)+C_k(-n_0)], \quad (19a)$$

$$\mathrm{i}\,\dot{C}_k(-n_0)=-\Omega\,[C_j(-n_0+1)+C_j(-n_0-1)], \quad (19b)$$

$$\mathrm{i}\,\underline{\dot{C}_j(-n_0-1)}=\varepsilon(n_0+1)\ C_j(-n_0-1) -\Omega\,[\underline{C_k(-n_0-2)}+C_k(-n_0)]. \quad (19c)$$

In the limit when ε is much larger than Ω, any nonvanishing diagonal element will dominate the time evolution. The corresponding amplitudes can be eliminated adiabaticaly [17] and we find that the probability will oscillate between the two amplitudes with $n=0$ and $-n_0$; this is a generalization of the pendellösung discussed earlier [13]. To obtain the correct result to lowest order in Ω, we need to decouple the equations for $n=1$ and $-(n_0+1)$; amplitudes outside this range acquire but little probability and can be neglected.

In the Bragg limit, we can consequently neglect all the terms *underlined* in (18) and (19). Inserting the solutions into the amplitude equations (18b) and (19b) we find the same frequency expression on the diagonal

$$D \equiv -\frac{\Omega^2}{\varepsilon}\left(\frac{1}{n_0+1}-\frac{1}{n_0-1}\right)=\frac{2\Omega^2}{\varepsilon(n_0^2-1)}. \tag{20}$$

The diagonal terms are of the form $\varepsilon n(n_0+n)$ and hence, going from $n=0$ to $n=-n_0$, we accumulate (n_0-1) factors of ε and two factors of $(n_0-1)!$; one set growing from $n=1$ and the other one decreasing from (n_0-1). We use n_0 steps and hence we get n_0 factors of Ω, each one switching the sign. The coupled equations we obtain are thus $(n_0>1)$

$$\mathrm{i}\frac{d}{dt}C_k(-n_0)=\frac{2\Omega^2}{\varepsilon(n_0^2-1)}C_k(-n_0) + \frac{(-\Omega)^{n_0}}{\varepsilon^{n_0-1}[(n_0-1)!]^2}C_1(0), \tag{21}$$

$$\mathrm{i}\frac{d}{dt}C_1(0)=\frac{2\Omega^2}{\varepsilon(n_0^2-1)}C_1(0) + \frac{(-\Omega)^{n_0}}{\varepsilon^{n_0-1}[(n_0-1)!]^2}C_k(-n_0). \tag{22}$$

Only the lowest order in Ω is retained in the coefficients. These equations are of the form

$$\mathrm{i}\dot{C}_k = D\,C_k - \tfrac{1}{2}K\,C_1$$

and

$$\mathrm{i}\dot{C}_1 = D\,C_1 - \tfrac{1}{2}K\,C_k \tag{23}$$

with the solution

$$C_1(t)=\mathrm{e}^{-\mathrm{i}Dt}\cos(\tfrac{1}{2}Kt)$$

and

$$C_k(t)=\mathrm{i}\,\mathrm{e}^{-\mathrm{i}Dt}\sin(\tfrac{1}{2}Kt), \tag{24}$$

where the initial condition $C_1(0)=1$ at $t=0$ has been used. In the probabilities the phase factors cancel and only the flipping at the frequency

$$|K|=\frac{2\Omega^{n_0}}{\varepsilon^{n_0-1}[(n_0-1)!]^2} \tag{25}$$

can be seen. However, when the diffractive pattern is used in an interferometric configuration, the outgoing beams may be mixed with some other component of the atomic beam which allows one to observe, e.g., the component

$$S \propto \cos\varphi\,\mathrm{Re}[C(-n_0)]+\sin\varphi\,\mathrm{Im}[C(-n_0)] \tag{26}$$

dependening on some angle φ of the mixing beam. Then the oscillation frequency D of (20) will show up, too. This is always of second order in Ω, whereas the order of the flipping frequency K is of higher order in the parameter (Ω/ε) as soon as $n_0>2$. Because this factor is small in the Bragg regime, we find the flipping frequency to be slow compared with the oscillation frequency D.

The case $n_0=1$ is a special situation not included in (21) and (22). Following the same procedure as above we find the coupled equations

$$\mathrm{i}\dot{C}_1(0)=-\frac{\Omega^2}{2\varepsilon}C_1(0)-\Omega C_2(-1)$$

and

$$\mathrm{i}\dot{C}_2(-1)=-\frac{\Omega^2}{2\varepsilon}C_2(-1)-\Omega C_1(0). \tag{27}$$

These are of the form (23), but now the flipping frequency equals Ω and the oscillation frequency D is but a small modulation. The resonances are found at $(\Omega\pm\Omega^2/2\varepsilon)$. In this case, as for all the odd cases, the resonance occurs between the ground state population (C_1) and the excited state population (C_2). Because the latter will decay by spontaneous emission, it may be difficult to observe such resonances in experiments.

The lowest order resonance between two ground state populations is the case $n_0=2$. This is a special situation because both D and K are of the same order and combine to give

$$C_1(0)=\exp\left(-\mathrm{i}\frac{2\Omega^2}{3\varepsilon}t\right)\cos(\Omega^2 t/\varepsilon) =\frac{1}{2}\left[\exp\left(\mathrm{i}\frac{\Omega^2}{3\varepsilon}t\right)+\exp\left(-\mathrm{i}\frac{5\Omega^2}{3\Theta}t\right)\right],$$

$$C_1(-2)=\mathrm{i}\exp\left(-\mathrm{i}\frac{2\Omega^2}{3\varepsilon}t\right)\sin(\Omega^2 t/\varepsilon) =\frac{1}{2}\left[\exp\left(\mathrm{i}\frac{\Omega^2}{3\varepsilon}t\right)-\exp\left(-\mathrm{i}\frac{5\Omega^2}{3\varepsilon}t\right)\right]. \tag{28}$$

For $n_0>2$ the frequency K is always less than D in the Bragg limit.

3 Properties of the Multiphoton Resonances

In order to investigate how distinctly and easily the multiphoton resonances can be seen, we have written a computer program that integrates the (8) numerically for any values of the parameters. In Fig. 3 we show the case $W_0=1.5\,\Omega$, when the momentum distribution spreads out and reassembles itself approximately after the time $(2\pi/W_0)$, see (12). from this expression we can also estimate the maximum momentum excursion to be

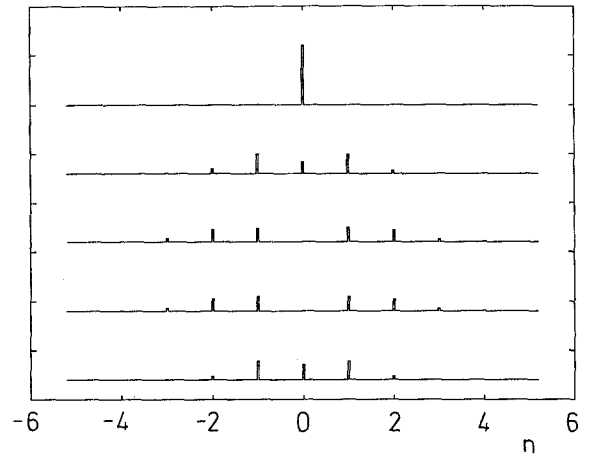

Fig. 3. Kapitza-Dirac scattering of atoms: The distribution of the probabilities $|C_i(n)|^2$ starting with the time $t=(1/\Omega)$ at the bottom. Going upwards we show the distribution at time intervals spaced by $(1/\Omega)$. The parameters are $\varepsilon=0.01\,\Omega$ and $W_0=1.5\,\Omega$. The distribution has reassembled itself at the time $(5/\Omega)$ close to the theoretical value $(2\pi/W_0)$. The initial distribution $|C_i(n)|^2=\delta_{n,0}$ at $t=0$ is not shown

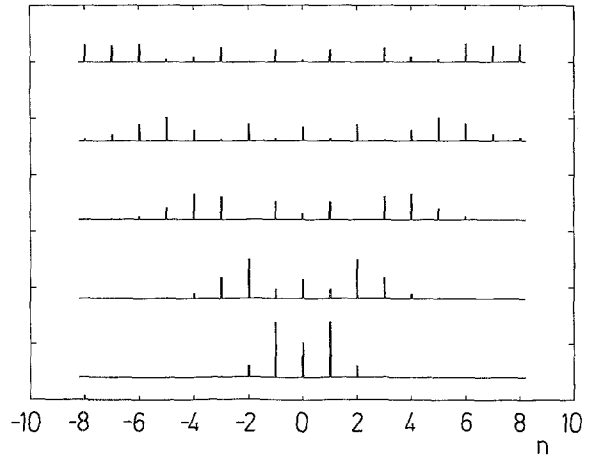

Fig. 4. Kapitza-Dirac scattering of atoms for the special case of orthogonal incidence, $W_0=0$. The other parameters are as in Fig. 3

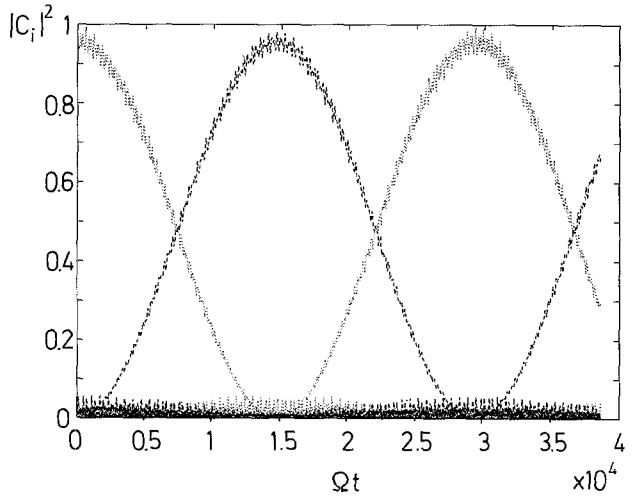

Fig. 5. The populations $|C_i(n)|^2$ of the momentum states as functions of the interaction time for a moderately adiabatic situation ($\varepsilon=2\,\Omega$). In this case the rapidly oscillating non-resonant amplitudes are still discernible in addition to the slowly oscillating probabilities of the two resonant states with $n=-n_0=-5$ and $n=0$

$(4\Omega/W_0)\simeq 2.7$, which agrees with the numerically obtained result.

In Fig. 4 we show the situation where the atoms hit the laser beam orthogonally ($W_0=0$). In this case, (12) predicts a linear spreading of the momentum distribution in accordance with the numerical result shown in Fig. 4. However, this trend will be broken by the accumulated Doppler shift when $\varepsilon>0$, but our integration has not been extended that far.

After the momentum distributions had been computed we Fourier-transformed them to obtain their spectral components. In the Bragg limit (13), the adiabatic approximation procedure presented above gives simple analytical results. In the interference variables (26) we expect to see the two frequencies $(D\pm\frac{1}{2}K)$; here we choose $\varphi=0$ and investigate the real part only. In the occupation probabilities for the states we find the frequencies $\pm K$, because the phase disappears and the frequency becomes doubled in the squares of the occupation probabilities (24).

We have investigated the first three resonances, $n_0=1$, 2, and 3 for various values of ε/Ω, which is the adiabaticity parameter. In addition, we have looked at one higher order resonance with $n_0=5$. In this case, the two frequencies differ by several orders of magnitude and some of the numerical results become less reliable as is discussed below. The general idea of Bragg flipping between the two resonant states is, however, still clearly discernible. Figure 5 shows the occupation probabilities of the momentum states for $n_0=5$ and $\varepsilon=2\Omega$. The two resonant states clearly display sinusoidal oscillations whereas all other probabilities remain insignificant as demanded by the adiabatic approximation. The main flipping frequency K emerges and all other oscillations are seen to be much faster.

In Fig. 6 we show the spectrum for $n_0=1$ and $\varepsilon=2\Omega$. This value is only marginally in the adiabatic regime, but the simple Bragg regime behaviour is still clearly seen. Of the frequency pair $(D\pm K/2)$, one becomes negative and crosses to the other side of the zero frequency, see Fig. 6a. Figure 6b shows directly the frequency K and also the zero component resulting from the squares of the trigonometric functions in (24).

Figure 7 shows the spectra for $n_0=2$ and $\varepsilon=10\,\Omega$. The adiabatic behaviour is well developed, and again, one component of the spectrum (Fig. 7a) crosses the zero frequency. Figure 8 shows the same result for the case $n_0=3$ and $\varepsilon=14\,\Omega$. The adiabatic behaviour is clearly seen and the frequency K can be obtained from the spectrum in Fig. 8b. This flipping frequency here is small as compared with D and causes only a small splitting around it as seen in Fig. 8a.

For the case $n_0=5$, we find the frequencies D and K to be of different orders of magnitude because of the factor $(\Omega/\varepsilon)^4/(4!)^2$ seen in (25). We show the spectra for $\varepsilon=6\Omega$ in Fig. 9. The ratio of the two frequences here is about 10^4 and no splitting of the frequency D is visible in Fig. 9a. It is consequently not possible to obtain a value for K from such a spectrum. The frequency K can, however, be determined from Fig. 9b, where the dependence on D is canceled.

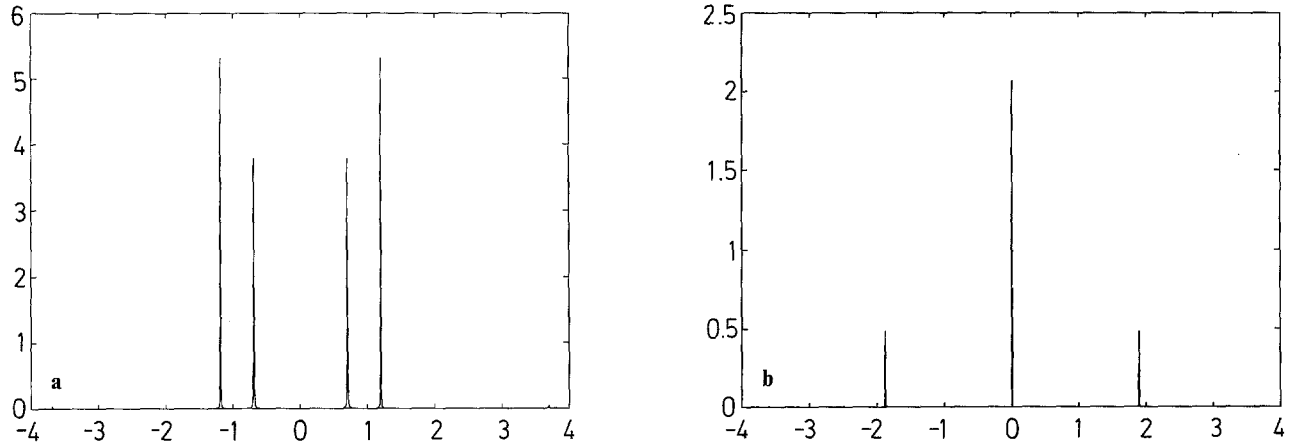

Fig. 6. **a** The power spectrum of $\mathrm{Re}[C_i(-n_0)]$ and **b** that of $|C_i(n)|^2$. The frequency is given as a multiple of Ω. The parameters are $n_0=1$ and $\varepsilon=2\,\Omega$

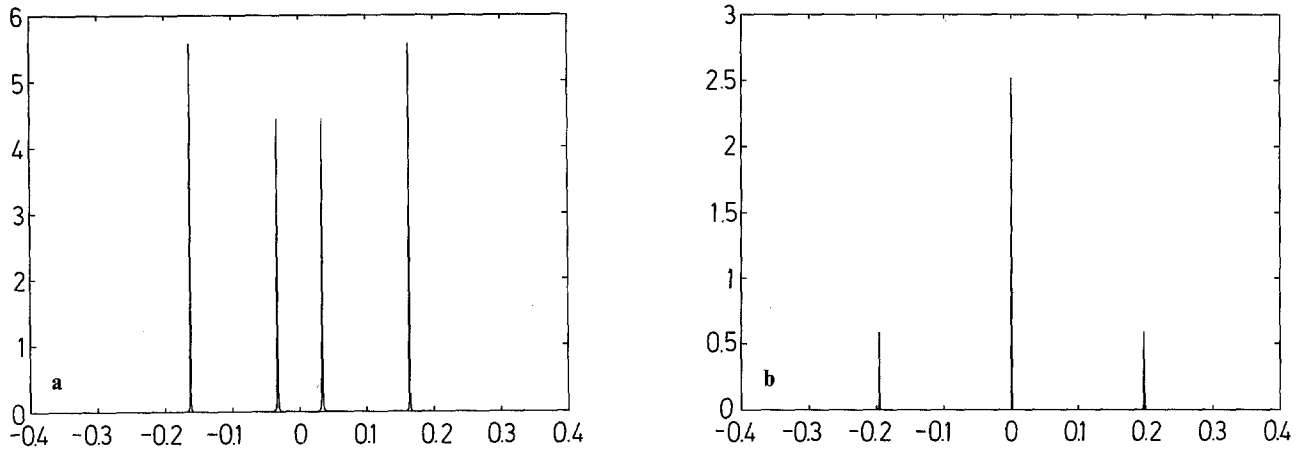

Fig. 7. The power spectra as in Fig. 6 for $n_0=2$ and $\varepsilon=10\,\Omega$

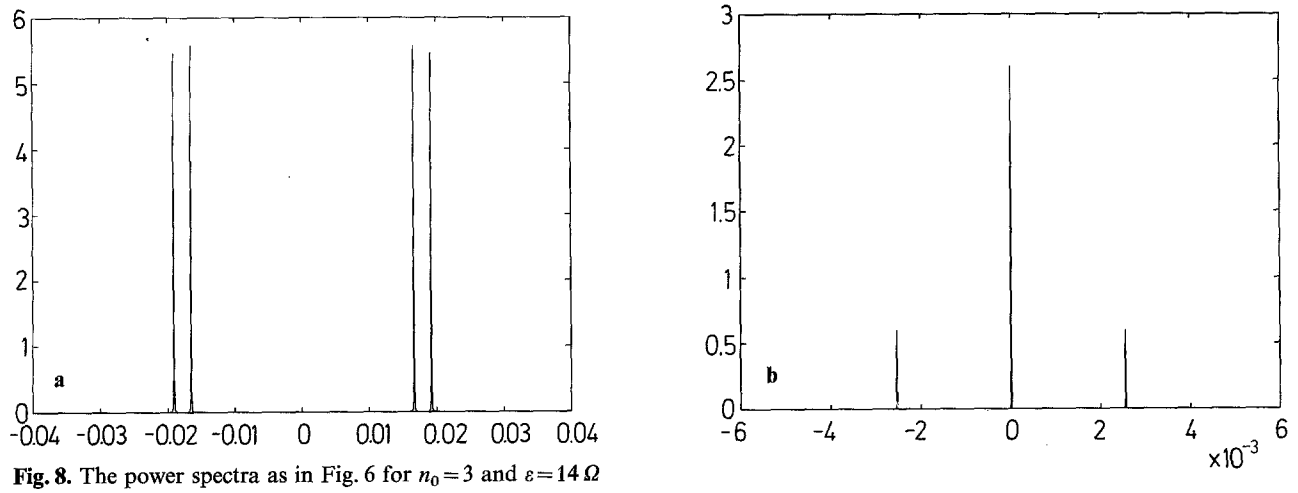

Fig. 8. The power spectra as in Fig. 6 for $n_0=3$ and $\varepsilon=14\,\Omega$

The results of our calculations are summarized in Table 1. We denote the two frequencies (20) and (25) by D_0 and K_0; these are the values obtained from the adiabatic approximation. The values denoted by D_1 and K_1 are obtained from the spectra of the real parts, i.e., Figs. 6a, 7a, 8a, and 9a. As already mentioned, no value for K_1 can be obtained for $n_0=5$. The spectra in Figs. 6b, 7b, 8b, and 9b give another estimate for the flipping frequency, here denoted K_2. The values are given as a multiple of Ω and the accuracy of the numerically obtained results is approximately one unit in the least significant digit given in the Table; it decreases rapidly with growing order n_0 because of the increasing difference between D and K.

From Table 1 we can conclude that the adiabatic behavious is very easy to observe. For all cases investigated the agreement with the adiabatic theory is rapidly improved when (ε/Ω) increases. Already $\varepsilon=6\Omega$

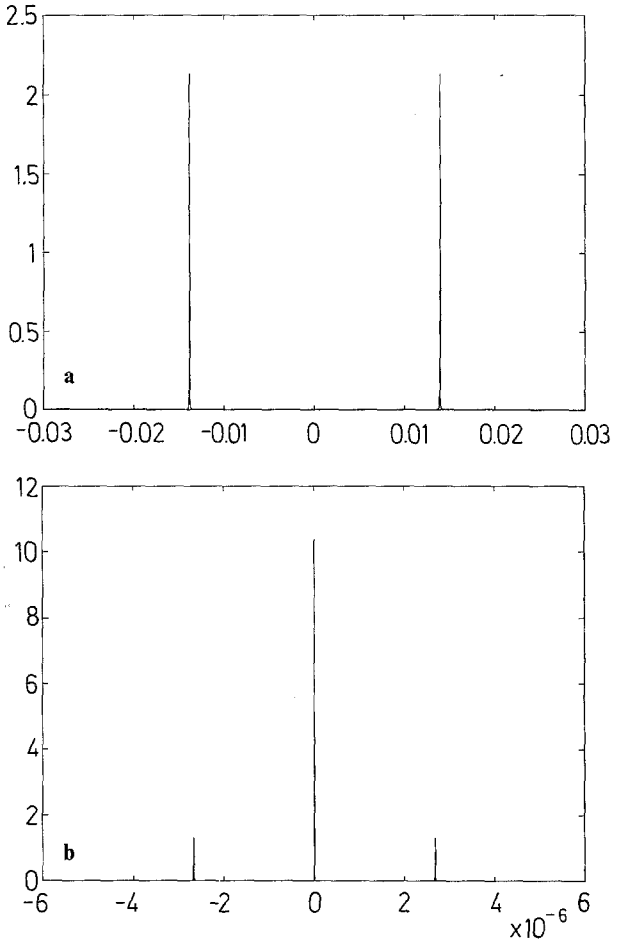

Fig. 9. The power spectra as in Fig. 6 for $n_0=5$ and $\varepsilon=6\,\Omega$

Table 1. Summary of results. All values are given in multiples of Ω. D_0 and K_0 follow from adiabatic theory. D_1 and K_1 follow from the spectrum of $\mathrm{Re}[C(-n_0)]$. K_2 follows from the spectrum of $|C(-n_0)|^2$.

$\frac{\varepsilon}{\Omega}=$		2	6	10	14
$n_0=1$	D_0	0.250	0.083	0.050	0.036
	D_1	0.250	0.082	0.051	0.039
	K_0	2.00	2.00	2.00	2.00
	K_1	1.87	1.98	1.98	1.98
	K_2	1.88	1.98	1.99	1.99
$n_0=2$	D_0	0.333	0.111	0.067	0.048
	D_1	0.213	0.103	0.065	0.047
	K_0	1.00	0.333	0.200	0.143
	K_1	0.75	0.316	0.195	0.141
	K_2	0.75	0.317	0.196	0.141
$n_0=3$	D_0	0.125	0.042	0.025	0.018
	D_1	0.190	0.042	0.025	0.018
	K_0	0.125	0.014	0.005	0.0026
	K_1	0.133	0.014	0.005	0.0025
	K_2	0.142	0.014	0.005	0.0025
$n_0=5$	D_0	0.042	0.014	0.0083	0.0060
	D_1	0.042	0.014	0.0083	0.0059
	K_0	0.220×10^{-3}	0.027×10^{-4}	0.03×10^{-5}	0.01×10^{-5}
	K_1	***	***	***	***
	K_2	0.21×10^{-3}	0.027×10^{-4}	0.03×10^{-5}	0.01×10^{-5}

*** = the value has not been obtained with sufficient accuracy

gives nearly perfect results. For $\varepsilon=14\Omega$ all cases give excellent agreement.

4 Discussion and Conclusion

In the discussion of atomic interferometric configurations the standing wave has become something of a prototype example. It does provide the atomic optics realization of gratings, beam splitters, and deflecting mirrors. In this paper we have discussed the various orders of scattering in the Bragg regime and compared their treatment with the multiphoton resonances seen in radio-frequency spectra. This analogy can be supported by the Doppleron interpretation introduced earlier in laser spectroscopy. The conservation of the kinetic energy of the atoms introduces the recoil energy as a frequency shift which gives the Dopplerons an anharmonic energy spectrum, see (8).

We have also carried out a numerical investigation to see how well the intuitive picture of flipping between resonant momentum states emerges from the exact theory. The conclusion is that the analytically obtained picture is very good in all parameter ranges investigated. The results are summarized in Table 1.

The order of the resonances is here determined by the integer n_0 defined in (16). When n_0 is odd, the one resonating state corresponds to the atom in its upper energy level and its detection may be hampered by the inevitable spontaneous decay out of this state. On the other hand, this decay may be utilized to observe the very process we are interested in. For even values of n_0, both resonating states correspond to the lower level; if this is a ground or metastable state it can be detected far away from the interaction region.

In this paper we have investigated only the case of resonant tuning of the laser. For a nonvanishing detuning Δ, the situation differs somewhat. If the integer n_0 of (17) is even, the resonance occurs between two ground state amplitudes and our treatment remains valid. A large value of Δ only aids in the adiabatic elimination of the upper state amplitudes. However, there appears the possibility to have other resonances, where the change of kinetic energy compensates the detuning. From (8) we find this to happen for

$$n_\pm = -\frac{1}{2\varepsilon}\left(W_0 \pm \sqrt{W_0^2-4\Delta\varepsilon}\right). \tag{29}$$

For $\varepsilon=0$, these were the Doppleron resonances discussed in [9]. When one value $n_\pm$ becomes an integer, a resonance occurs. Even both may be integers, and it is possible that n_0 is an integer for the same parameters. Thus we may have two or three resonant amplitudes occurring simultaneously, and then the treatment becomes more involved than the one presented in this paper. The adiabatic elimination program can still be carried out, and judging from the results of the present work, the adiabatic approximation is expected to be good in these cases, too.

In this paper we have regarded the electromagnetic field as a classical quantity. In most experimental

situations, this is the appropriate limit and the phenomena we have explored here are not influenced by the quantum nature of the field. In fact, it is perfectly straightforward to extend our treatment to the case of a quantized standing wave. The coupling constants in (8) will become functions of the occupation number N of the photon states, viz. $\Omega \propto \sqrt{N}$. The adiabatic elimination procedure can still be carried out, see [16], for the analogous radio-frequency case, and the powers of Ω in (21) and (22) will be replaced by products of differing values of N. Only when n_0 becomes comparable with the number of photons in the beam, quantum effects will become observable. This may, on the other hand, be an interesting region to investigate owing to the insights it can give into the nature of the quantized fields, cf. [18].

References

1. E. Arimondo, H. Lew, T. Oka: Phys. Rev. Lett **43**, 753 (1979)
2. V.A. Grinchuk, A.P. Kazantsev, E.F. Kuzin, M.L.Nagaeva, G.A. Ryabenko, G.I. Surdutovich, V.P. Yakovlev: Sov. Phys.-JETP **59**, 56 (1981)
3. P.E. Moskowitz, P.L. Gould, S.R. Atlas, D. Pritchard: Phys. Rev. Lett. **51**, 370 (1983)
4. P.J. Martin, P.L. Gould, B.G. Oldaker, A.H. Miklich, D.E. Pritchard: **A36**, 2495 (1987)
   P.J. Martin, B.G. Oldaker, A.H. Miklich, D.E. Pritchard: Phys. Rev. **60**, 515 (1988)
5. E. Arimondo, A. Bambini, S. Stenholm: Phys. Rev. **A24**, 898 (1981)
6. C. Tanguy, S. Reynaud, C. Cohen-Tannoudji: J. Phys. B **17**, 4623 (1984)
7. M. Wilkens, E. Schumacher, P. Meystre: Opt. Commun. **86**, 34 (1991)
8. P.L. Gould, P.J. Martin, G.A. Ruff, R.E. Stoner, J.-L. Picque, D.E. Pritchard: Phys. Rev. **A43**, 585 (1991)
9. E. Kyrölä, S. Stenholm: Opt. Commun. **22**, 123 (1977); **30**, 37 (1979)
10. J. Winter: Compt. Rend. Acad. Sci. **241**, 375 (1955)
11. C. Cohen-Tannoudji: In *Cargèse Lectures in Physics*, Vol. 2, ed. by M. Levy (Gordon and Breach, New York 1968)
12. S. Haroche: Ann. Phys. (Paris) **6**, 189, 327 (1971)
13. P. Meystre, E. Schumacher, E.M. Wright: Ann. Phys. **7**, 48, 141 (1991)
14. N.P. Bigelow, M.G. Prentiss: Phys. Rev. Lett. **65**, 555 (1990)
    J.J. Tollett, J. Chen, J.G. Story, N.W.M. Ritchie, C.C. Bradley, R.G. Hulet: Phys. Rev. Lett. **65**, 559 (1990)
15. B. Macke: Opt. Commun. **28**, 131 (1979)
16. S. Stenholm: Phys. Rev. **C6**, 2 (1973)
17. L. Allen, C.R. Stroud, Jr.: Phys. Rev. **91**, 1 (1982)
18. B.W. Shore, P. Meystre, S. Stenholm: J. Opt. Soc. Am. **B8**, 903 (1991) P. Meystre, E. Schumacher, S. Stenholm: Opt. Commun. **73**, 443 (1989)